

## THE HALO MASS FUNCTION FROM EXCURSION SET THEORY. II. THE DIFFUSING BARRIER

MICHELE MAGGIORE<sup>1</sup> AND ANTONIO RIOTTO<sup>2,3</sup>

*Draft version April 28, 2022*

### ABSTRACT

In excursion set theory the computation of the halo mass function is mapped into a first-passage time process in the presence of a barrier, which in the spherical collapse model is a constant and in the ellipsoidal collapse model is a fixed function of the variance of the smoothed density field. However,  $N$ -body simulations show that dark matter halos grow through a mixture of smooth accretion, violent encounters and fragmentations, and modeling halo collapse as spherical, or even as ellipsoidal, is a significant oversimplification. In addition, the very definition of what is a dark matter halo, both in  $N$ -body simulations and observationally, is a difficult problem. We propose that some of the physical complications inherent to a realistic description of halo formation can be included in the excursion set theory framework, at least at an effective level, by taking into account that the critical value for collapse is not a fixed constant  $\delta_c$ , as in the spherical collapse model, nor a fixed function of the variance  $\sigma$  of the smoothed density field, as in the ellipsoidal collapse model, but rather is itself a stochastic variable, whose scatter reflects a number of complicated aspects of the underlying dynamics. Solving the first-passage time problem in the presence of a diffusing barrier we find that the exponential factor in the Press-Schechter mass function changes from  $\exp\{-\delta_c^2/2\sigma^2\}$  to  $\exp\{-a\delta_c^2/2\sigma^2\}$ , where  $a = 1/(1 + D_B)$  and  $D_B$  is the diffusion coefficient of the barrier. The numerical value of  $D_B$ , and therefore the corresponding value of  $a$ , depends among other things on the algorithm used for identifying halos. We discuss the physical origin of the stochasticity of the barrier and, from recent  $N$ -body simulations that studied the properties of the collapse barrier, we deduce a value  $D_B \simeq 0.25$ . Our model then predicts  $a \simeq 0.80$ , in excellent agreement with the exponential fall off of the mass function found in  $N$ -body simulations, for the same halo definition. Combining this result with the non-markovian corrections computed in paper I of this series, we derive an analytic expression for the halo mass function for gaussian fluctuations and we compare it with  $N$ -body simulations.

*Subject headings:* cosmology:theory — dark matter:halos — large scale structure of the universe

### 1. INTRODUCTION

The relation between the linear density perturbations at early time and the abundance of virialized dark matter halos at the present epoch is an extremely relevant one in modern cosmology. In particular, primordial non-gaussianities leave an imprint on the abundance and on the clustering properties of the most massive objects, such as galaxy clusters, which form out of rare fluctuations (Matarrese et al. 1986; Grinstein & Wise 1986; Lucchin et al. 1988; Moscardini et al. 1991; Koyama et al. 1999; Matarrese et al. 2000; Robinson & Baker 2000; Robinson et al. 2000). These observational signatures are potentially detectable by various planned large-scale galaxy surveys.

From the theoretical side, the challenge is to compute the number density of dark matter halos of mass  $M$ ,  $n(M)$ , in terms of the statistical properties of the primordial density field. The formation and evolution of dark matter halos is a highly complicated process, and its full dynamical complexity can only be studied by  $N$ -body simulations. As revealed by  $N$ -body simulations, halos grow through a messy mixture of violent encounters, smooth accretion and fragmentation (see Springel et al. (2005) and the related movies at <http://www.mpa-garching.mpg.de/galform/millennium/>).

Still, some analytic understanding of halo formation is highly desirable, both for obtaining a better physical intuition, and for the flexibility under changes of models or parameters

(such as cosmological model, shape of the non-Gaussianities, etc.) which is the advantage of analytical results over very timing consuming numerical simulations. Presently the best available analytical technique is based on Press-Schechter (PS) theory (Press & Schechter 1974) and its extension known as excursion set theory (Bond et al. 1991) and is able to reproduce, at least qualitatively, several properties of dark matter halos seen in  $N$ -body simulations, such as their conditional and unconditional mass function, halo accretion histories, merger rates and halo bias (see Zentner (2007) for a recent review). However excursion set theory describes the collapse as spherical, in its original formulation, or as ellipsoidal, in the extension due to Sheth & Tormen (1999). This is clearly an important oversimplification of the actual complex dynamics and, as a result, while qualitatively the prediction of excursion set theory agree with  $N$ -body simulations, at the quantitative level there are important discrepancies, and dynamical evidence in favor of excursion set theory, at least in its present formulation, is quite weak (Robertson et al. 2008). A related concern is that numerical simulations show that there is not a good correspondence between peaks in the initial density field and collapsed halos (see Katz et al. (1993) for an early result).

In this paper we continue the investigation of excursion set theory that we started in Maggiore & Riotto (2009a) (hereafter paper I). In paper I we have shown how excursion set theory can be put on firmer mathematical grounds, and we have been able to take into account analytically the non-markovian contribution to the evolution of the smoothed density field, due to the use of a tophat filter in coordinate space. In the present paper we turn to a reexamination of the physics be-

<sup>1</sup> Département de Physique Théorique, Université de Genève, 24 quai Ansermet, CH-1211 Genève, Switzerland

<sup>2</sup> CERN, PH-TH Division, CH-1211, Genève 23, Switzerland

<sup>3</sup> INFN, Sezione di Padova, Via Marzolo 8, I-35131 Padua, Italy

hind excursion set theory and we propose a generalization of the theory, based on the idea that the critical value for collapse of the smoothed density field should be treated as a stochastic variable. We discuss how this stochasticity originates physically and we show that supplementing excursion set theory with a diffusing barrier allows us to capture at least some of the complexity of the actual halo formation process, which is lost in the spherical or elliptical collapse model.

Our notation is as in paper I. Namely, we consider the density contrast  $\delta(\mathbf{x}) = [\rho(\mathbf{x}) - \bar{\rho}]/\bar{\rho}$ , where  $\bar{\rho}$  is the mean mass density of the universe and  $\mathbf{x}$  is the comoving position, and we smooth it on some scale  $R$ , defining

$$\delta(\mathbf{x}, R) = \int d^3x' W(|\mathbf{x} - \mathbf{x}'|, R) \delta(\mathbf{x}'), \quad (1)$$

with a filter function  $W(|\mathbf{x} - \mathbf{x}'|, R)$ . For gaussian fluctuations, the statistical properties of the fundamental density field  $\delta(\mathbf{x})$  are embodied in its power spectrum  $P(k)$ , defined by

$$\langle \tilde{\delta}(\mathbf{k}) \tilde{\delta}(\mathbf{k}') \rangle = (2\pi)^3 \delta_D(\mathbf{k} + \mathbf{k}') P(k), \quad (2)$$

where  $\tilde{\delta}(\mathbf{k})$  are the Fourier modes of  $\delta(\mathbf{x})$ . From this one finds the variance  $\sigma^2(R)$  of the smoothed density field

$$\sigma^2(R) \equiv \langle \delta^2(R) \rangle. \quad (3)$$

If we smooth the density field with a tophat filter function in coordinate space, the mass  $M$  associated to a smoothing radius  $R$  is  $M = (4/3)\pi R^3 \bar{\rho}$ , and we can consider  $\sigma$  as a function of  $M$ , rather than of  $R$ . The ambiguities involved in assigning a mass  $M$  to a smoothing scale  $R$  when one uses a different filter function have been discussed in detail in paper I.

The halo mass function  $dn/dM$  can be written as

$$\frac{dn(M)}{dM} = f(\sigma) \frac{\bar{\rho}}{M^2} \frac{d \ln \sigma^{-1}(M)}{d \ln M}. \quad (4)$$

In Press-Schechter theory (Press & Schechter 1974) and in excursion set theory (Bond et al. 1991) the function  $f(\sigma)$  is predicted to be

$$f_{\text{PS}}(\sigma) = \left(\frac{2}{\pi}\right)^{1/2} \frac{\delta_c}{\sigma} e^{-\delta_c^2/(2\sigma^2)}, \quad (5)$$

where  $\delta_c \simeq 1.686$  is the critical value in the spherical collapse model. This result can be extended to arbitrary redshift  $z$  by reabsorbing the evolution of the variance into  $\delta_c$ , so that  $\delta_c$  in the above result is replaced by  $\delta_c(z) = \delta_c(0)/D(z)$ , where  $D(z)$  is the linear growth factor. However, eq. (5) is valid only if the density is smoothed with a sharp filter in momentum space, and in this case there is no unambiguous way of assigning a mass to a region of radius  $R$ . In paper I we have been able to extend this result to a tophat filter in coordinate space. In this case the computation is considerably more difficult. In fact, when the density perturbation is smoothed with a sharp filter in momentum space,  $\delta(R)$  obeys a Langevin equation with respect to the ‘‘pseudotime’’ variable  $S(R) \equiv \sigma^2(R)$ , with a Dirac delta noise. This means that the dynamics is markovian, and that the probability  $\Pi(\delta, S)$  that the density contrast reaches the value  $\delta$  at ‘‘time’’  $S$  satisfies a Fokker-Planck (FP) equation, with an ‘‘absorbing barrier’’ boundary condition  $\Pi(\delta_c, S) = 0$ . For different filters the dynamics becomes non-markovian, and  $\Pi(\delta, S)$  no longer satisfies a local diffusion equation such as the FP equation. In paper I we have been able to formulate the problem of the computation of  $\Pi(\delta, S)$  in terms of a path integral with boundaries and we

have found that the result can be split into a ‘‘markovian’’ and a ‘‘non-markovian’’ part. The markovian part simply gives back eq. (5), where now  $\sigma^2(M)$  is the variance computed with the tophat filter in coordinate space, while the non-markovian terms can be evaluated perturbatively. To first order, we found

$$f(\sigma) = (1 - \kappa) \left(\frac{2}{\pi}\right)^{1/2} \frac{\delta_c}{\sigma} e^{-\delta_c^2/(2\sigma^2)} + \frac{\kappa}{\sqrt{2\pi}} \frac{\delta_c}{\sigma} \Gamma\left(0, \frac{\delta_c^2}{2\sigma^2}\right), \quad (6)$$

where

$$\kappa(R) \equiv \lim_{R' \rightarrow \infty} \frac{\langle \delta(R') \delta(R) \rangle}{\langle \delta^2(R') \rangle} - 1 \simeq 0.4592 - 0.0031 R, \quad (7)$$

$R$  is measured in  $\text{Mpc}/h$ ,  $\Gamma(0, z)$  is the incomplete Gamma function, and the numerical value of  $\kappa(R)$  is computed assuming a  $\Lambda$ CDM model compatible with the WMAP 5yrs data and a tophat filter function in coordinate space. Observe that for a sharp filter in momentum space,  $\langle \delta(R') \delta(R) \rangle = \langle \delta^2(\max(R, R')) \rangle$  so  $\kappa(R)$ , as defined by the first equality in eq. (7), vanishes.

However, neither eq. (5) nor eq. (6) perform well when compared to cosmological  $N$ -body simulation. Indeed, PS theory predicts too many low-mass halos, roughly by a factor of two, and too few high-mass halos: at  $\sigma^{-1} = 3$  (high masses correspond to small values of  $\sigma$ ), PS theory is already off by a factor  $\mathcal{O}(10)$ . The mass function given in eq. (6), in the interesting mass range, is everywhere lower than the PS prediction and therefore, while it improves the agreement at low masses, it gives an even worse result at high masses, see Fig. 9 of paper I. Thus, it is clear that some crucial physical ingredient is still missing in the model. This is not surprising at all, given the use of the simplified spherical collapse model. In the large mass limit the result cannot be improved by turning to the ellipsoidal collapse model since, as we will review in the next section, at large masses the barrier for ellipsoidal collapse reduces to the one for spherical collapse. The aim of this paper is to show that treating the collapse barrier as a stochastic variable allows us to capture some of the complicated physics that is missed by the spherical or ellipsoidal collapse model, and we will see that this modification gives just the required behavior in the large mass limit.

The organization of the paper is as follows. In Section 2, after recalling how a moving barrier emerges from the ellipsoidal collapse model (Sheth et al. 2001), we discuss in detail the physical motivations for the introduction of a stochastic barrier. In Section 3 we compute the halo mass function with a diffusing barrier, both for the markovian case and including the non-markovian corrections, and in Section 4 we compare our prediction for the mass function with  $N$ -body simulations. Section 5 contains our conclusions.

## 2. THE ELLIPSOIDAL COLLAPSE BARRIER AND THE DIFFUSING BARRIER

The fact that extended PS theory gives a qualitatively correct answer but fails at the quantitative level has led many authors either to resort to fits to the  $N$ -body simulations, see e.g. Sheth & Tormen (1999); Sheth et al. (2001); Jenkins et al. (2001); Warren et al. (2006); Tinker et al. (2008); Pillepich et al. (2008); Grossi et al. (2009), or to look for improvements of the spherical collapse model. Sheth et al. (2001) took into account the fact that actual halos are triaxial (Bardeen et al. 1986; Bond & Myers 1996), and that the collapse of halos occurs along the principal axes. As a result, the ellipsoidal

collapse barrier  $B$  acquires a  $\sigma$ -dependence,

$$B(\sigma) \simeq \delta_c \left[ 1 + 0.47 \left( \frac{\sigma}{\delta_c} \right)^{1.23} \right]. \quad (8)$$

Physically this reflects the fact that low-mass halos (which corresponds to large  $\sigma$ ) have larger deviations from sphericity and significant shear, that opposes collapse. Therefore low-mass halos require an higher density to collapse. In contrast, very large halos are more and more spherical, so their effective barrier reduces to the one for spherical collapse.

It is apparent that the use of a moving barrier of the form (8), by itself, cannot improve the agreement with  $N$ -body simulations in the large mass limit since, for large masses (which correspond to  $\sigma \rightarrow 0$ ),  $B(S)$  reduces to the value for the spherical collapse and therefore we get back the incorrect prediction of extended PS theory. More generally, since the barrier is receding away from its initial location  $\delta_c$ , it is more difficult for the smoothed density perturbation to reach it, at any  $\sigma$ , so the use of eq. (8) simply gives a halo mass function which is everywhere smaller than the PS prediction.

In order to improve the agreement between the prediction from the excursion set method with an ellipsoidal collapse and the  $N$ -body simulations, Sheth et al. (2001) found that it was necessary to introduce a new parameter  $a$  (which, when they require that their mass function fits the GIF simulation, turns out to have the value  $a \simeq 0.707$ , i.e.  $\sqrt{a} \simeq 0.84$ ) and postulate that the form of the barrier is rather

$$B(\sigma) \simeq \sqrt{a} \delta_c \left[ 1 + 0.47 \left( \frac{\sigma}{\sqrt{a} \delta_c} \right)^{1.23} \right]. \quad (9)$$

It is important to stress that, in Sheth et al. (2001), the parameter  $a$  is not derived from the dynamics of the ellipsoidal collapse. Rather on the contrary, the ellipsoidal collapse model predicts  $a = 1$  because in the limit  $\sigma \rightarrow 0$  the barrier must reduce to that of spherical collapse. In Sheth et al. (2001) the parameter  $a$  is just introduced by hand in order to fit the  $N$ -body simulations.

To clarify the origin of this parameter, it is useful to recall how eq. (8) emerges. One considers the gravitational collapse of a homogeneous ellipsoid, as in Bond & Myers (1996). Denoting by  $\phi$  the peculiar gravitational potential at the location of an ellipsoidal patch, the deformation tensor is  $\partial_i \partial_j \phi$ , and its eigenvalues  $\lambda_1, \lambda_2, \lambda_3$  (ordered so that  $\lambda_1 \leq \lambda_2 \leq \lambda_3$ ) characterize the shape of the ellipsoid. In the linear regime, using Poisson equation, the density contrast  $\delta$  is given by the trace of the deformation tensor, so  $\delta = \lambda_1 + \lambda_2 + \lambda_3$ . In a gaussian random field, the probability distribution of the eigenvalues is known, and is given by (Doroshkevich (1970); see Lam et al. (2009) for a recent generalization to the non-Gaussian case)

$$p_\sigma(\lambda_1, \lambda_2, \lambda_3) = \frac{15^3}{8\pi\sqrt{5}\sigma^6} (\lambda_2 - \lambda_1)(\lambda_3 - \lambda_2)(\lambda_3 - \lambda_1) \times \exp \left\{ -\frac{3I_1^2}{\sigma^2} + \frac{15I_2}{2\sigma^2} \right\}, \quad (10)$$

where  $I_1 \equiv \lambda_1 + \lambda_2 + \lambda_3 = \delta$  and  $I_2 \equiv \lambda_1 \lambda_2 + \lambda_2 \lambda_3 + \lambda_1 \lambda_3$ . By integrating out  $\lambda_1$  and  $\lambda_2$  at fixed  $\delta$ , with the constraint  $\lambda_1 \leq \lambda_2 \leq \lambda_3$ , one verifies that  $\delta$  has a gaussian distribution, with variance  $\sigma^2$ . Rather than using the three eigenvalues as independent variables one can use  $\delta$ , together with the ellipticity  $e$  and prolateness  $p$ , defined by

$$e = \frac{\lambda_3 - \lambda_1}{2\delta}, \quad (11)$$

$$p = \frac{\lambda_1 + \lambda_3 - 2\lambda_2}{2\delta}. \quad (12)$$

From  $p_\sigma(\lambda_1, \lambda_2, \lambda_3) d\lambda_1 d\lambda_2 d\lambda_3$  one can derive the distribution probability  $g_\sigma(e, p | \delta) de dp$  for  $e, p$  at fixed  $\delta$ . The result is (Bardeen et al. 1986; Sheth et al. 2001)

$$g_\sigma(e, p | \delta) = \frac{1125}{\sqrt{10}\pi} e(e^2 - p^2) \left( \frac{\delta}{\sigma} \right)^5 \exp \left\{ -\frac{5}{2} \frac{\delta^2}{\sigma^2} (3e^2 + p^2) \right\}. \quad (13)$$

To define a barrier one needs a criterium for collapse in the ellipsoidal case. In Sheth et al. (2001) collapse along each axis is stopped so that the density contrast at virialization is the same as in the spherical collapse model, i.e. 179 times the critical density of the universe. Given this criterium, the critical value for collapse in the ellipsoidal model,  $\delta_{\text{ell}}$ , is a function of  $e, p$ , well approximated by the implicit relation (Sheth et al. 2001)

$$\frac{\delta_{\text{ell}}(e, p)}{\delta_c} \simeq 1 + \beta \left[ 5(e^2 \pm p^2) \frac{\delta_{\text{ell}}^2(e, p)}{\delta_c^2} \right]^\gamma, \quad (14)$$

where  $\delta_c$  is the critical value for spherical collapse, the plus (minus) sign holds for  $p$  negative (positive),  $\beta \simeq 0.47$  and  $\gamma \simeq 0.615$ . The barrier (8) follows if one replaces  $e$  and  $p$  with their most probable values according to the distribution  $g(e, p | \delta)$ , which are  $\bar{e} = \sigma / (\delta \sqrt{5})$  and  $\bar{p} = 0$  (and furthermore one replaces  $\delta_{\text{ell}}(e, p)$ , on the right-hand side of eq. (14), with  $\delta$ ).

As we already mentioned, this barrier always stays above the spherical collapse barrier at  $\delta_c$ , and reduces to the spherical collapse one for  $\sigma = 0$ , i.e. for large masses. For our purpose, it is however important to note that this result only holds if  $e$  and  $p$  are replaced by their most probable values  $\bar{e}$  and  $\bar{p}$ . For generic values of  $e$  and  $p$  the critical value for collapse can be either higher or lower than  $\delta_c$ . This results in a "fuzzy" threshold (Audit et al. 1997; Lee & Shandarin 1998; Sheth et al. 2001), with a probability distribution that extends even to values smaller than  $\delta_c$ . To compute the variance of the barrier due to this effect we use a slightly more accurate expression for the critical value of the ellipsoidal collapse as a function of the eigenvalues  $\lambda_i$  (Sandvik et al. 2006),

$$\delta_{\text{ell}}(\lambda_1, \lambda_2, \lambda_3) = \delta_c \left[ 1 + \alpha_1 (\lambda_2 - \lambda_1)^{\alpha_2} + \alpha_3 (2\lambda_3 - \lambda_2 - \lambda_1)^{\alpha_4} \right], \quad (15)$$

where  $\alpha_1 \simeq 0.2809$ ,  $\alpha_2 = 1.3557$ ,  $\alpha_3 \simeq 0.070$ ,  $\alpha_4 \simeq 1.41205$ .<sup>4</sup> We stress that this expression for the critical value of  $\delta$  was found in Sandvik et al. (2006) requiring an accurate representation of the ellipsoidal collapse of Bond & Myers (1996), and not by fitting to  $N$ -body mass functions. The average value of this barrier is

$$B_{\text{ell}}(\sigma) \equiv \langle \delta_{\text{ell}}(\lambda_1, \lambda_2, \lambda_3) \rangle = \int_{-\infty}^{\infty} d\lambda_3 \int_{-\infty}^{\lambda_3} d\lambda_2 \int_{-\infty}^{\lambda_2} d\lambda_1 \delta_{\text{ell}}(\lambda_1, \lambda_2, \lambda_3) p_\sigma(\lambda_1, \lambda_2, \lambda_3), \quad (16)$$

where  $p_\sigma(\lambda_1, \lambda_2, \lambda_3)$  is the probability distribution given in eq. (10). In Fig. 1 we compare this expression for  $B_{\text{ell}}(\sigma)$  with the expression given in (8). We see that they provide two similar representation of the average barrier for ellipsoidal collapse. The variance of  $B_{\text{ell}}(\sigma)$  is given by

<sup>4</sup> As in eq. (8), we are considering the barrier at  $z = 0$ , when the linear growth factor  $D(z) = 1$ . The expression for generic  $z$  is obtained by rescaling  $\delta_c \rightarrow \delta_c / D(z)$  and  $\lambda_i \rightarrow \lambda_i D(z)$ , see eq. (18) of Sandvik et al. (2006).

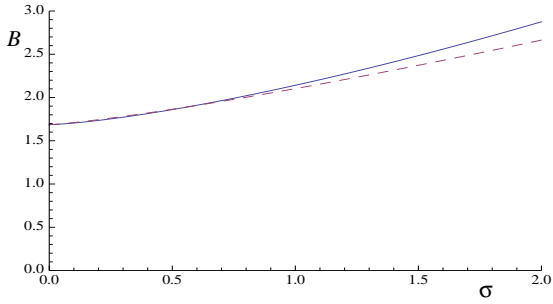


FIG. 1.— Two possible representations for the ellipsoidal collapse barrier as a function of  $\sigma$ . The red dashed line is the barrier given in eq. (8). The blue solid line is the function  $B_{\text{ell}}(\sigma)$  obtained from eqs. (15) and (16).

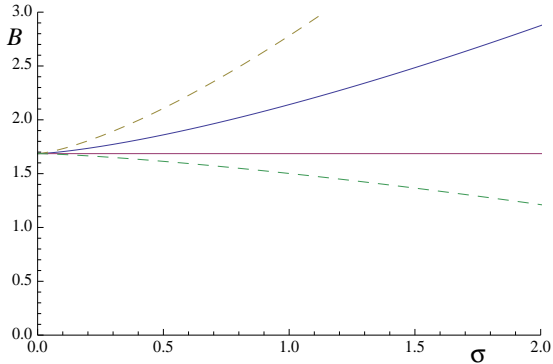


FIG. 2.— The function  $B_{\text{ell}}(\sigma)$  (blue solid line), together with the curves  $B_{\text{ell}}(\sigma) \pm 3\Sigma_{B_{\text{ell}}}(\sigma)$  (dashed lines). The horizontal red solid line is the spherical collapse barrier  $B = \delta_c$ .

$$\begin{aligned} \Sigma_{B_{\text{ell}}}^2(\sigma) &\equiv \langle [\delta_{\text{ell}}(\lambda_1, \lambda_2, \lambda_3) - B_{\text{ell}}(\sigma)]^2 \rangle \\ &\simeq \delta_c^2 [0.00805\sigma^{2\alpha_2} + 0.00489\sigma^{2\alpha_4} + 0.00305\sigma^{\alpha_2+\alpha_4}], \end{aligned} \quad (17)$$

where again the averages have been computed using the distribution (10). In Fig. 2 we compare  $B_{\text{ell}}(\sigma)$  with the curves  $B_{\text{ell}}(\sigma) \pm 3\Sigma_{B_{\text{ell}}}(\sigma)$ . We see that a fluctuation of the barrier at the  $3\Sigma_{B_{\text{ell}}}$  level can bring the threshold for collapse well below the constant value  $\delta_c$  derived from the spherical collapse model (see also Fig. 7 of Sheth et al. (2001)).

This result already makes it clear that, as a matter of principle, the critical value for collapse is unavoidably a stochastic variable. However, the fluctuations of the barrier discussed above by no means exhaust all possible sources of stochasticity in the actual physical problem. For instance, halos are subject to tidal effects due to their environment, which also results in a distribution of values for the collapse barrier (Desjacques 2008). More generally, modeling dark matter halos as smooth and homogeneous ellipsoids characterized by the eigenvalues  $\lambda_i$ , even when taking into account their distribution probability, is still a significant oversimplification. For instance, a patch that is collapsing might have significant non-linear substructures, whose presence influences its critical value for collapse. All these effects contribute to the scatter of the values of the threshold for collapse.

Last but not least, the very definition of what is a dark matter halo is a non-trivial problem both in numerical simulations and observationally (for cluster observations, see Jeltema et al. (2005) and references therein). In simulations, halos are usually identified either through a Friends-of-Friends (FOF) algorithm, or using spherical overdensity (SO) finders. However actual halos are triaxial, rather than spherical,

and often messier than that, and there is nothing fundamental or rigorous in either choice, both being largely a matter of convenience. FOF halo finders track isodensity profiles and might be more relevant for Sunayev-Zeldovich or weak lensing, while SO finders may be more relevant for cluster work. Searching for halos using for instance a spherical overdensity finder, when halos are at best triaxial and often more irregular, introduces a further source of statistical fluctuations, both in the number count of halo, and in the assignment of the mass. A similar concern is that the exact definition of a virialized halo depends on the what one means exactly by “virialized”.

So in the end, in a given  $N$ -body simulation, each patch of the initial density field that eventually collapses to form a halo at a given epoch, has a smoothed overdensity that does not have in general exactly the value predicted by the ellipsoidal collapse model, but rather fluctuates around it with fluctuations that are determined by various factors, such as the distributions of the eigenvalues of the deformation tensor, the details of the halo finder algorithm, or other details related to the environment, the presence of non-linear substructures, etc., as discussed above.

Motivated by these considerations, we propose in this paper to extend excursion set theory by considering a first-passage time problem in the presence of a barrier that fluctuates stochastically. Given that the fluctuations in the collapse threshold depend, among other things, on the exact details of the halo definition (halo finder, virialization criterium, etc.), the mass function computed from excursion set theory with such a stochastic barrier will depend on these details, too. This is a positive aspect because the actual halo mass function obtained from  $N$ -body simulations depends on the halo finder (White 2001). For instance, with FOF finders the mass function depends on the link-length used, and in particular the value  $a \simeq 0.707$  given in eq. (9) holds for a link-length equal to 0.2 times the mean inter-particle separation (Sheth et al. 2001).<sup>5</sup> When halos are identified with a SO finder, the mass function depends on the value chosen for the overdensity  $\Delta$ , see e.g. Tinker et al. (2008). These effects cannot be reproduced by excursion set theory with a barrier which is fixed uniquely by the dynamics of the spherical or ellipsoidal collapse, and which therefore is insensitive to these details. In this paper we explore whether the use of a stochastic barrier allows us to incorporate into excursion set theory, at least at the level of an effective description, a part of the stochasticity intrinsic to the actual physical problem of halo formation, and due both to the complicated underlying dynamics and to the choices that one has made when giving an operative definition of dark matter halos.

Ideally, one would like to compute theoretically the fluctuation properties of the barrier. For some effect, such as that due to the distribution of eigenvalues of the deformation tensor, this is possible, as we saw in eq. (17). Unfortunately, other effects such as the scatter of the barrier due to the details of the halo finder (which, as it will turn out, give a contribution that dominates over that in eq. (17)) are much more difficult to predict theoretically. We will therefore take a more phenomenological approach. We will consider a barrier that performs a random walk with a diffusion coefficient  $D_B$ . At least at a first level of description, all our ignorance of the

<sup>5</sup> Observe that, for this link length, a sizable fraction of halos have major non-spherical substructures and a significant contribution to the halo mass arises from outside the “virial” radius (Lukic et al. 2009). This underlines again the importance of the details of the definition of what is a halo.

details of the dynamics of halo formation is buried into this coefficient. Solving the first-passage time problem with such a barrier we will find that the net effect is that in the halo mass function predicted by Press-Schechter or excursion set theory the exponential factor changes from  $\exp\{-\delta_c^2/(2\sigma^2)\}$  to  $\exp\{-a\delta_c^2/(2\sigma^2)\}$  (and more generally we must replace everywhere  $\delta_c \rightarrow \delta_c\sqrt{a}$ ), where

$$a = \frac{1}{1+D_B}, \quad (18)$$

see Section 3. This is just the replacement that was postulated in Sheth et al. (2001); Sheth & Tormen (1999) in order to fit the data. We therefore discover that the Sheth and Tormen (ST) mass function (at least in the large mass limit), is just the mass function obtained by excursion set theory with a diffusing barrier.

Having obtained a physical understanding of the parameter  $a$  that appears in the ST mass function, one can ask whether it is possible to go beyond the approach in Sheth & Tormen (1999); Sheth et al. (2001), where  $a$  is simply treated as a fitting parameter, and try to predict it, by computing the diffusion coefficient  $D_B$ . Given that a first-principle computation of  $D_B$  seems difficult, in Section 4 we will turn to  $N$ -body simulations themselves. We will see that recent numerical studies of the properties of the collapse threshold allows us to deduce the value of  $D_B$ . Given this input we will then compare our prediction (18) to the slope of the exponential fall off of the mass function, and more generally (including in the halo mass function also the non-markovian corrections computed in paper I) we will compare our analytic form for the mass function to the numerical data. Even if in this way we must use an input from  $N$ -body simulations themselves, still the comparison is quite non-trivial, since the relation (18) is a specific prediction of our model.

### 3. THE HALO MASS FUNCTION IN THE PRESENCE OF THE DIFFUSING BARRIER

In order to illustrate the idea in a simple mathematical setting, we consider a barrier that fluctuates over the constant spherical collapse barrier  $B = \delta_c$ . In the large mass limit the ellipsoidal collapse barrier reduces to the spherical collapse barrier, so we expect that this approximation should be adequate for computing the effect of a stochastic barrier on the high-mass tail of the halo mass function. We also consider a barrier  $B$  that fluctuates in such a way that its mean root square fluctuation  $\Sigma_B$  depends linearly on the variance of the smoothed density field  $\sigma(R)$ ,

$$\Sigma_B(\sigma(R)) \equiv \langle (B - \langle B \rangle)^2 \rangle^{1/2} = \sigma(R)\sqrt{D_B}, \quad (19)$$

where  $D_B$  is a numerical coefficient. This choice is partly motivated by mathematical simplicity. Furthermore, we will see in Section 4 that there is some evidence from  $N$ -body simulations that for small  $\sigma(R)$  the barrier diffuses just as in eq. (19).

This form of the barrier corresponds to a brownian motion. Recall in fact that, if a particle performs a one-dimensional brownian motion, its position  $x(t)$  has a variance given by  $\langle (x(t) - x_0)^2 \rangle^{1/2} = \sqrt{Dt}$ , where  $D$  is the diffusion coefficient. In the excursion set method  $S(R) = \sigma^2(R)$  plays the role of a ‘‘pseudotime’’ variable, so eq. (19) means that the collapse barrier performs a brownian motion around its initial position  $\langle B \rangle$ , with a diffusion coefficient  $D_B$ . We will refer to the model in which the barrier’s scatter behaves as in eq. (19) as a ‘‘diffusing barrier’’. As we will see below, the first passage time problem in the presence of a diffusing barrier can be

solved analytically, so eq. (19) provides at least a useful toy model for understanding the effect of a more general stochastic barrier. We emphasize however that the idea that we are proposing is more general, and can in principle be implemented for a generic functional form of the barrier  $B(\sigma)$  and of its fluctuation  $\Sigma_B(\sigma)$ , although the associated first-passage time problem becomes more complicated, and might require the numerical generation of an ensemble of trajectories using Monte Carlo simulations, as in Bond et al. (1991).

Intuitively, we can understand why a diffusing barrier can help to reproduce the numerical  $N$ -body results. We are interested in events, corresponding to cluster masses, that arise from rare fluctuations, on the far tails of the probability distribution. For instance at  $\sigma^{-1} = 3$ , the PS theory prediction for  $f(\sigma)$  is about  $10^{-5}$ , and we are searching for a mechanism that brings this number up to the observed value of about  $10^{-4}$ . Even if, on average, a barrier has equal probabilities of fluctuating toward values lower than  $\delta_c$  as toward values higher than  $\delta_c$ , still the fluctuations of the barrier toward lower values can have a much more significant effect (consider for instance what happens to a dam if on a rare occasion it is lowered). In fact, this is true even if most of the fluctuation were above  $\delta_c$ , and only rare fluctuations were below  $\delta_c$  which, as we will see, is the case when we consider fluctuations over the ellipsoidal collapse barrier, see also Fig. 2. In the analogy with the dam, rare occasional lowerings of the dam can produce substantial flooding, even if many more fluctuations rather raise it.

To verify formally this intuition, we neglect at first the non-markovian corrections due to the filter, discussed in paper I. We denote by  $\Pi(B(0), B; \delta(0), \delta; S)$  the joint probability that, at ‘‘time’’  $S$ , the barrier has reached by diffusion the value  $B$ , starting from the initial value  $B(0) = \delta_c$ , while the density contrast has reached the value  $\delta$ , starting from the initial value  $\delta(0) = 0$ . In the markovian case the probability distribution obeys a Fokker-Planck equation. The fact that the ‘‘particle’’ described by  $\delta(S)$  and the barrier  $B(S)$  both diffuse independently means that the joint probability distribution satisfies the two-dimensional FP equation

$$\frac{\partial \Pi}{\partial S} = \frac{D}{2} \frac{\partial^2 \Pi}{\partial \delta^2} + \frac{D_B}{2} \frac{\partial^2 \Pi}{\partial B^2}. \quad (20)$$

In our case the diffusion coefficient of  $D = 1$ , see e.g. eq. (20) of paper I, while  $D_B$  is the diffusion coefficient of the barrier. To solve this equation it is convenient to introduce a ‘‘time’’ variable  $t = S/\delta_c^2$ , and the variables

$$x_1 = \frac{\delta_c - B}{\delta_c \sqrt{D_B}}, \quad (21)$$

$$x_2 = \frac{\delta_c - \delta}{\delta_c}, \quad (22)$$

so eq. (20) becomes

$$\frac{\partial \Pi}{\partial t} = \frac{1}{2} \frac{\partial^2 \Pi}{\partial x_1^2} + \frac{1}{2} \frac{\partial^2 \Pi}{\partial x_2^2}. \quad (23)$$

In term of these variables the barrier starts at  $x_1(0) = 0$  while the ‘‘particle’’ starts at  $x_2(0) = 1$ . The boundary condition is that  $\Pi(B(0), B; \delta(0), \delta; S)$  vanishes when  $\delta(S) = B(S)$ , i.e.  $\Pi(x_1(0), x_1; x_2(0), x_2; t)$  vanishes when  $\sqrt{D_B}x_1 = x_2$ . We define  $\theta$  from  $\sqrt{D_B} = \tan \theta$ , so we have a two-dimensional FP equation with the boundary condition that  $\Pi$  vanishes on the line  $x_1 = x_2 \cot \theta$ , see Fig. 3. This problem can be solved by the method of images (Redner 2001), and the result is given

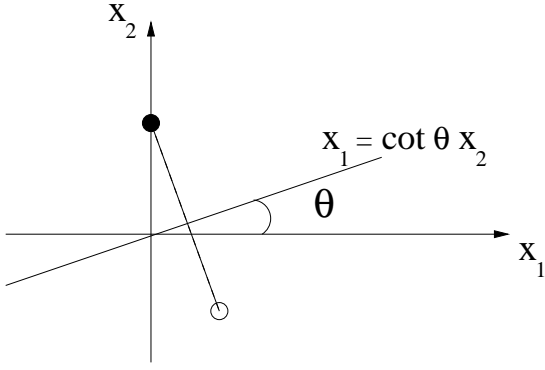


FIG. 3.— Mapping of the scaled density perturbation and collapse barrier coordinates in one dimension to the plane  $(x_1, x_2)$ . The initial position is in  $(x_1 = 0, x_2 = 1)$  (black dot) and its image point is in  $(x_1 = \sin 2\theta, x_2 = -\cos 2\theta)$  (white dot).

by a gaussian centered on  $(x_1 = 1, x_2 = 0)$  minus a gaussian centered on the image point  $(x_1 = \sin 2\theta, x_2 = -\cos 2\theta)$ ,

$$\begin{aligned} \Pi^{\text{gm}}(x_1(0) = 0, x_1; x_2(0) = 1, x_2; t) \\ = \frac{1}{2\pi t} \left[ e^{-[x_1^2 + (x_2 - 1)^2]/2t} - e^{-[(x_1 - \sin 2\theta)^2 + (x_2 + \cos 2\theta)^2]/2t} \right], \end{aligned} \quad (24)$$

where, as in paper I, we added to  $\Pi$  the superscript “gm” to remind that this is the solution for gaussian fluctuation with a markovian dependence on the smoothing scale

The probability density for the scaled density perturbation to be at the position  $x_2$  is the integral of the two-dimensional density over the accessible range of the scaled collapse barrier coordinate  $x_1$ ,

$$\begin{aligned} \Pi^{\text{gm}}(x_2, t) &= \int_{-\infty}^{x_2 \cot \theta} dx_1 \Pi^{\text{gm}}(x_1; x_2; t) \\ &= \frac{1}{2\sqrt{2\pi t}} \left[ e^{-(x_2 - 1)^2/2t} \text{Erfc} \left( -\frac{x_2 \cot \theta}{\sqrt{2t}} \right) \right. \\ &\quad \left. - e^{-(x_2 + \cos 2\theta)^2/2t} \text{Erfc} \left( \frac{\sin 2\theta - x_2 \cot \theta}{\sqrt{2t}} \right) \right], \end{aligned} \quad (25)$$

where  $\text{Erfc}(z)$  is the complementary error function and the initial conditions  $x_1(0) = 0$  and  $x_2(0) = 1$  are understood. Restoring the original variables  $S, \delta(S)$  and  $B(S)$ , and using  $\Pi(\delta_0; \delta; S)d\delta = \Pi(x_2(0); x_2; t)|dx_2|$  where  $|dx_2| = d\delta/\delta_c$ , we get

$$\begin{aligned} \Pi^{\text{gm}}(\delta, S) &= \frac{1}{2\sqrt{2\pi S}} \left\{ e^{-\delta^2/(2S)} \text{Erfc} \left[ -\frac{\cot \theta}{\sqrt{2S}} (\delta_c - \delta) \right] \right. \\ &\quad \left. - e^{-(2\delta_c \cos^2 \theta - \delta^2)/(2S)} \text{Erfc} \left[ \frac{\delta_c \sin 2\theta - (\delta_c - \delta) \cot \theta}{\sqrt{2S}} \right] \right\}, \end{aligned} \quad (26)$$

where the initial condition  $\delta_0 = 0$  is understood. The limit of non-diffusing barrier is  $D_B \rightarrow 0^+$ , so  $\theta \rightarrow 0^+$  and  $\cot \theta \rightarrow +\infty$ . Recalling that  $\text{Erfc}(z) \rightarrow 2$  as  $z \rightarrow -\infty$ , we see that in the limit  $D_B \rightarrow 0^+$  we recover the standard result of excursion set theory with a static barrier of Bond et al. (1991).

In Fig. 4 we compare this function, for a diffusion coefficient  $D_B = 0.25$ , with the static barrier case. Observe that, when  $D_B = 0$ , the distribution function vanishes for  $\delta \geq \delta_c$ ,<sup>6</sup> while for finite  $D_B$  it is non-zero for all values of  $\delta$ . Of course,

<sup>6</sup> This only holds because, for the markovian term, we can work directly in the continuum limit. As we discussed in paper I, if we compute  $\Pi$  summing over trajectories defined discretizing time in steps  $\epsilon$ , there are finite  $\epsilon$  corrections and  $\Pi(\delta, S)$  non longer vanishes for  $\delta \geq \delta_c$ , even for the static barrier.

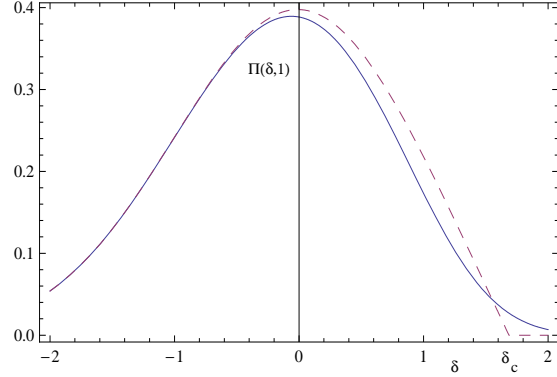


FIG. 4.— The function  $\Pi^{\text{gm}}(\delta, S)$  with  $D_B = 0.25$  (blue solid line) compared to the standard excursion set result, i.e.  $\Pi^{\text{gm}}(\delta, S)$  with  $D_B = 0$  (violet dashed line), as functions of  $\delta$ , for  $S = 1$ .

this reflects the fact that the barrier can in principle diffuse to arbitrarily large values of  $\delta$ .

The markovian contribution to the first crossing rate is

$$\mathcal{F}^{\text{gm}}(S) = - \int_{-\infty}^{\infty} d\delta \frac{\partial \Pi^{\text{gm}}(\delta, S)}{\partial S}. \quad (27)$$

The evaluation of this expression can be simplified observing that  $\partial/\partial S$ , when acting on  $(2\pi S)^{-1/2} \exp\{-\delta^2/(2S)\}$ , is the same as  $(1/2)\partial^2/\partial\delta^2$ , and integrating twice by parts  $\partial^2/\partial\delta^2$ . We then find

$$\mathcal{F}^{\text{gm}}(S) = \frac{\delta_c}{\sqrt{2\pi(1+D_B)} S^{3/2}} \exp \left\{ -\frac{\delta_c^2}{2(1+D_B)S} \right\}. \quad (28)$$

The function  $f(\sigma)$  is obtained from the first crossing rate using  $f(\sigma) = 2\sigma^2 \mathcal{F}(\sigma^2)$ , see e.g. Section 2 of paper I, so we get

$$f^{\text{gm}}(\sigma) = \left( \frac{2}{\pi} \right)^{1/2} \frac{\sqrt{a} \delta_c}{\sigma} e^{-a\delta_c^2/(2\sigma^2)}, \quad (29)$$

where

$$a = \frac{1}{1+D_B}. \quad (30)$$

This is the crucial result of this section. We see that the effect of the diffusing barrier is that the exponential factor in the halo mass function changes from  $\exp\{-\delta_c^2/(2\sigma^2)\}$  to  $\exp\{-a\delta_c^2/(2\sigma^2)\}$ , with  $a$  given by eq. (30), and more generally everywhere in the mass function  $\delta_c \rightarrow \delta_c \sqrt{a}$ . This is exactly the modification which was postulated *ad hoc* in Sheth et al. (2001).

In fact, even if the expression for  $\Pi^{\text{gm}}(\delta, S)$  given in eq. (26) is interesting by itself, the result for the first-crossing rate could have been obtained directly, without even computing explicitly  $\Pi^{\text{gm}}(\delta, S)$ , simply by observing that the problem involving a barrier with coordinate  $x_1$  and diffusing with a diffusion coefficient  $D_1$ , and a particle with coordinate  $x_2$ , diffusing with a diffusion coefficient  $D_2$ , can be mapped into a one-degree of freedom problem, introducing the relative coordinate  $x = x_2 - x_1$ . The resulting stochastic motion is governed by an effective diffusion coefficient  $D_{\text{eff}} = D_1 + D_2$  (Redner 2001). This point can be easily understood considering a Langevin equation for the barrier coordinate  $x_1$ ,

$$\dot{x}_1 = \eta_1(t), \quad (31)$$

with

$$\langle \eta_1(t) \eta_1(t') \rangle = D_1 \delta(t - t'), \quad (32)$$

and a Langevin equation for the particle coordinate  $\dot{x}_2 = \eta_2(t)$  with  $\langle \eta_2(t)\eta_2(t') \rangle = D_2 \delta(t-t')$ . Then the relative coordinate  $x = x_2 - x_1$  satisfies  $\dot{x} = \eta(t)$  with  $\eta(t) = \eta_2(t) - \eta_1(t)$  and, if  $\eta_1(t)$  and  $\eta_2(t)$  are uncorrelated,

$$\begin{aligned} \langle \eta(t)\eta(t') \rangle &= \langle \eta_1(t)\eta_1(t') \rangle + \langle \eta_2(t)\eta_2(t') \rangle \\ &= (D_1 + D_2) \delta(t-t'), \end{aligned} \quad (33)$$

showing that the relative coordinate diffuses with an effective diffusion coefficient  $D_1 + D_2$ . In our case  $D_1 = D_B$  and  $D_2 = 1$ .

We have repeated the above analysis including the non-markovian corrections due to a tophat filter in coordinate space, to first order, using the results obtained in paper I. The explicit computation is performed in Appendix A. The result is

$$f(\sigma) = (1 - \tilde{\kappa}) \left( \frac{2a}{\pi} \right)^{1/2} \frac{\delta_c}{\sigma} e^{-a\delta_c^2/(2\sigma^2)} + \frac{\tilde{\kappa}\delta_c\sqrt{a}}{\sigma\sqrt{2\pi}} \Gamma \left( 0, \frac{a\delta_c^2}{2\sigma^2} \right), \quad (34)$$

where

$$\tilde{\kappa} = \frac{\kappa}{1 + D_B}. \quad (35)$$

This is our result for the halo mass function. We hasten to add that this result only holds in the large mass limit, otherwise we must consider fluctuations over the ellipsoidal barrier, rather than over the constant spherical constant barrier, and furthermore we have considered a specific form of the barrier variance, corresponding to a random walk. We now turn to a comparison of our model with  $N$ -body simulations.

#### 4. COMPARISON WITH $N$ -BODY SIMULATIONS

The variance of the collapse barrier in  $N$ -body simulations has been recently studied in Robertson et al. (2008) (see also Dalal et al. (2008)). For each halo identified in their  $N$ -body simulations at  $z = 0$ , they calculated the center-of-mass of the halo particles at their positions in the linear field at  $z \simeq 10^2$  and used the density field, smoothed with a tophat filter in real space, to compute the overdensity within a given lagrangian radius  $R$ . This overdensity is then linearly extrapolated to  $z = 0$ . They find that the distribution of such smoothed linear overdensities  $B(\sigma)$ , at fixed  $\sigma$ , is approximately log-normal in shape with a width  $\Delta_B$  given by

$$\Delta_B \simeq 0.3\sigma. \quad (36)$$

In a log-normal distribution one has

$$\Sigma_B \equiv \langle (B - \langle B \rangle)^2 \rangle^{1/2} = \left( e^{\Delta_B^2} - 1 \right)^{1/2} \langle B \rangle, \quad (37)$$

and in our case, for small  $\sigma$ ,  $\langle B \rangle \simeq \delta_c \simeq 1.68$ . Observe that eq. (37) is consistent with our estimate (17). In fact, eq. (17) only includes the scatter due to the fluctuations of the eigenvalues, so it is a lower bound on the actual scatter of the barrier that, as we discussed in Section 2, can in principle receive contributions from many other effects. As we see from Fig. 5 the variance given by eq. (37) is indeed always above that given by eq. (17).

In a  $\Lambda$ CDM model,  $\sigma(M)$  is such that, for values of  $M$  corresponding to cluster of galaxies,  $0.3\sigma(M) \ll 1$ . For instance,  $\sigma(M) = 1$  for  $M \simeq 10^{14} M_\odot h^{-1}$ , while  $\sigma(M) = 0.6$  for  $M \simeq 10^{15} M_\odot h^{-1}$  (see e.g. Fig. 1 of the review Zentner (2007)). Therefore in the high-mass range  $\Delta_B$  is small and we can expand eq. (37), obtaining

$$\Sigma_B \simeq \langle B \rangle \Delta_B \simeq 0.3\delta_c\sigma. \quad (38)$$

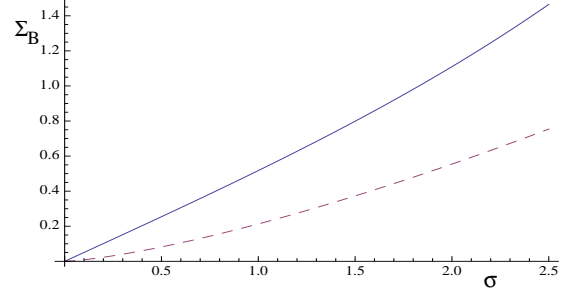


FIG. 5.— The variance of the barrier  $\Sigma_B$  from eq. (37) (blue solid line) compared to the estimate (17) (violet dashed line).

The inclusion of an overall drift of the barrier, such as that in eq. (8), as well as higher order terms in the expansion of the exponential in eq. (37), provides terms of higher order in  $\sigma$ , which are subleading in the large-mass regime.

Equation (38) has exactly the form of the diffusing barrier given in eq. (19), with a diffusion coefficient

$$D_B \simeq (0.3\delta_c)^2 \simeq 0.25. \quad (39)$$

In this case our model predicts a relation, given by eq. (30), between the diffusion coefficient  $D_B$  of the barrier and the slope of the exponential of the halo mass function in large mass limit, i.e. we predict

$$a = \frac{1}{1 + D_B} \simeq 0.80. \quad (40)$$

The value (39) has been deduced from the  $N$ -body simulations of Robertson et al. (2008), where halos were identified with a  $\Delta = 200$  spherical overdensity algorithm. We therefore must compare our prediction with the value of  $a$  obtained under the same conditions. This can be obtained from Tinker et al. (2008), where the same numerical simulation was used to study the halo mass function (and its deviations from universality, see below). The authors fit their result with a fitting function

$$f(\sigma) = A_T \left[ \left( \frac{\sigma}{b_T} \right)^{-a_T} + 1 \right] e^{-c_T/\sigma^2} \quad (41)$$

and, for a spherical overdensity  $\Delta = 200$ , they find  $A_T = 0.186$ ,  $a_T = 1.47$ ,  $b_T = 2.57$  and  $c_T \simeq 1.19$ . We add a subscript  $T$ , which stands for Tinker et al., to distinguish for instance their parameter  $a_T$  from our parameter  $a$ . A first indication of the agreement of our prediction with the above fitting formula can be obtained by comparing the respective exponential cutoff. In terms of their parameter  $c_T$ , our parameter  $a$  is given by the combination  $2c_T/\delta_c^2$ . Using their value  $c_T \simeq 1.19$ , one has  $2c_T/\delta_c^2 \simeq 0.837$ , in good agreement with the value (40). This agreement is a non-trivial result. It is true that, to get eq. (40), we used an input from the same  $N$ -body simulation, namely the scatter of the values of the threshold for collapse, from which we deduced the diffusion coefficient  $D_B$  of the barrier. However, given this input our model makes a non-trivial prediction for the numerical value of the parameter  $a$  that appears in the halo mass function. This is very different from fitting  $a$  directly to the  $N$ -body simulations. In principle, the prediction  $a = 1/(1 + D_B)$  could have given rise to a value of  $a$  very different from the one extracted directly from  $N$ -body simulations, and this would have falsified the diffusing barrier model.

Of course, given that the functional forms of  $f(\sigma)$  in eqs. (34) and (41) are different (which also implies that the

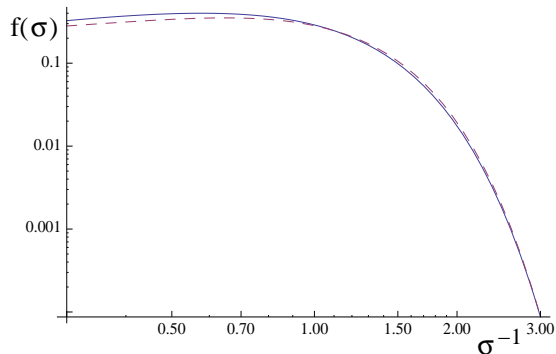


FIG. 6.— Our prediction for  $f(\sigma)$  given in eq. (34) (blue solid line) compared to the fit to  $N$ -body simulations given by eq. (41) (violet dashed line), in a log-log scale.

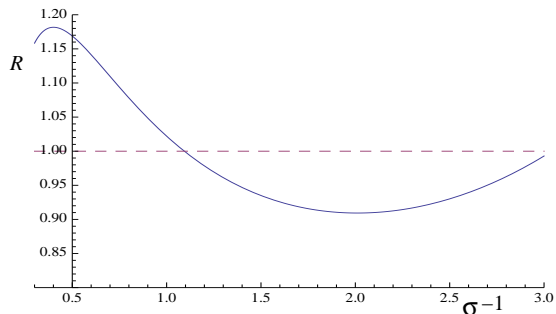


FIG. 7.— The ratio  $R$  between our prediction (34) for  $f(\sigma)$  and the fit to  $N$ -body simulations given by eq. (41) (blue solid line). The dashed line marks the line  $R = 1$ .

normalization constant  $A_T$  in eq. (41) is not exactly the same as the overall factor that we have in front of the exponential in eq. (34)), the proper way of performing an accurate comparison is not in terms of the location of the exponential cutoff, but rather directly in terms of the full functions  $f(\sigma)$ . In Fig. 6 we compare our prediction for  $f(\sigma)$ , given by eq. (34), to the function (41) representing the fit to the  $N$ -body simulation. Observe that the vertical axis ranges over more than three orders of magnitudes.

To make a more detailed comparison in Fig. 7 we plot, on a linear-linear scale, the ratio  $R$  between our prediction for  $f(\sigma)$  and the Tinker et al. fit to  $N$ -body simulations given in eq. (41). We see that for all values of  $\sigma^{-1} \geq 0.3$  the discrepancy between our analytic result and the fit to the  $N$ -body simulation is smaller than 20%, and for  $\sigma^{-1} \geq 1$  it is smaller than 10%. Considering that our result comes from an analytic model of halo formation with no tunable parameter (the parameter  $a$  is fixed once  $D_B$  is given, and we do not have the right to tune it), while eq. (41) is simply a fit to the data with four free parameters, we think that this result is quite encouraging. The numerical accuracy is actually the best that one could have hoped for, considering for instance that we have neglected second-order non-markovian corrections. From eq. (34) we see that, in the computation of the non-markovian effect due to the tophat filter in coordinate space in the presence of a diffusing barrier, the actual expansion parameter is  $\tilde{\kappa} = \kappa / (1 + D_B)$  which, using eq. (7) with  $R = 10$  Mpc and  $D_B \simeq 0.25$ , has a numerical value  $\tilde{\kappa} \simeq 0.34$ . Therefore the second-order non-markovian corrections, which are proportional to  $\tilde{\kappa}^2$ , are expected to be of order 10%. Furthermore, as we move toward lower masses the effect of the ellipsoidal barrier must become important, while eq. (34) has been ob-

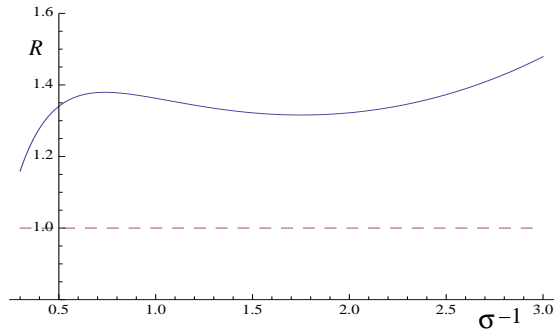


FIG. 8.— The ratio  $R$  between our prediction (34) for  $f(\sigma)$  and the fit to  $N$ -body simulations given by eq. (41) (blue solid line), setting  $\kappa = 0$ . The dashed line marks the line  $R = 1$ .

tained using the spherical collapse model, and the variance of the barrier  $\Sigma_B$  shown in Fig. (5) (solid line) has been approximated by a straight line in eq. (38), which again is only valid at small  $\sigma$ .

In Fig. 8 we show the result that one obtains for the ratio  $R$  if one includes the diffusing barrier but neglects the non-markovian corrections due to the tophat filter in coordinate space, i.e. if one sets  $\kappa = 0$  in eq. (34). We see that the agreement degrades, and the discrepancy becomes of order 30-50%. Thus, while the largest part of the improvement, compared to PS theory, comes from the introduction of a diffusing barrier (recall that PS theory, which predicts  $a = 1$ , is off by one order of magnitude in the high-mass limit, see e.g. Fig. 1 of paper I), still for an accurate computation it is important to include the non-markovian corrections due to the tophat filter in coordinate space. Observe also that, in the large mass limit, the term proportional to the incomplete Gamma function in eq. (34) is subleading, and the effect of the filter is basically to reduce the overall numerical factor, compared to PS theory, by a factor  $1 - \tilde{\kappa}$ . Note that in the ST mass function the numerical value of the overall constant is fixed by hand, by imposing the normalization condition that all the mass ends up in virialized objects. In our case, in contrast, the mass function comes out automatically with the correct normalization, as we already showed in Section 5.4 of paper I. The derivation given in eqs. (126)-(128) of paper I goes through trivially when  $\delta_c \rightarrow \delta_c \sqrt{a}$ , so the term proportional to the incomplete Gamma function in eq. (34) ensures that the mass function is properly normalized, when the amplitude of the term proportional to  $\exp\{-a\delta_c^2/(2\sigma^2)\}$  is reduced by a factor  $1 - \tilde{\kappa}$ .

## 5. CONCLUSIONS

In this paper we have proposed a generalization of excursion set theory, based on the idea that the threshold for collapse should be treated as a stochastic variable, fluctuating around the ellipsoidal collapse barrier (or, in the large mass limit, around the spherical collapse barrier). We have seen that fluctuations in the threshold arise naturally from a number of physical effects. For instance, even within the highly simplified description in which a halo is modeled as a smooth and homogeneous ellipsoid, fluctuations in the collapse barrier arise from the fact that the eigenvalues of its deformation tensor are stochastic variables, governed by a distribution probability. Only when one averages over this probability distribution one recovers a barrier which is a fixed function of the variance  $\sigma^2(R)$  of the smoothed density field. Otherwise, as already discussed in Audit et. al. (1997); Lee & Shandarin

(1998); Sheth et al. (2001) one has a "fuzzy barrier" which fluctuates around the ellipsoidal collapse value, with fluctuations that can occasionally bring the critical value for collapse even below the spherical collapse value  $\delta_c$ , see e.g. Fig. 2. As we have discussed, many other effects, such as the details of the halo finder, the environment, or the presence of non-linear substructures, contribute to these fluctuations.

For mathematical simplicity in this paper we have restricted ourselves to a barrier that performs a diffusive motion, with diffusion constant  $D_B$ , around the constant value given by spherical collapse. We expect this to be a good approximation in the large mass limit. For such a barrier we have found that the first-passage time problem can be elegantly solved, and leads to a very simple result. Namely, in the mass function one must replace  $\delta_c \rightarrow \sqrt{a}\delta_c$ , where  $a = 1/(1+D_B)$ . The replacement  $\delta_c \rightarrow \sqrt{a}\delta_c$  is just the modification that was postulated in Sheth et al. (2001), in order to fit the results of  $N$ -body simulations. The diffusing barrier model therefore offers a physical understanding of this modification of the PS mass function.

We have then combined our diffusing barrier model with the non-markovian corrections due to a tophat filter in coordinate space computed in paper I, and we have presented an analytic expression for the halo mass function, valid for large masses. This result can be compared with existing  $N$ -body simulations. We have inferred the value of  $D_B$  from the results presented in Robertson et al. (2008), and given  $D_B$  our model predicts the corresponding value of  $a$  for the same simulation. Our mass function, with  $a$  fixed in this way, is then compared to the corresponding  $N$ -body simulations in Figs. 6–7. The agreement is better than 20% for all  $\sigma^{-1} \geq 0.3$  (corresponding approximately to halo masses  $M \gtrsim 10^{11} M_\odot/h$ ) and better than 10% for all  $\sigma^{-1}$  in the interval  $1 \leq \sigma^{-1} \leq 3$  (corresponding approximately to halo masses from  $M \sim 10^{14} M_\odot/h$  to  $M \sim 10^{15} M_\odot/h$ ).

We conclude with an assessment of what can be obtained from excursion set theory, when it is combined with a diffusing barrier model, and with a discussion of possible improvements of the model. First of all one should stress that this theoretical model, using relatively simple ingredients, investigates a very complex phenomenon such as halo formation. It is therefore encouraging that it nevertheless provides an analytic result for the halo mass function that agrees with the  $N$ -body data with a precision better than 20% over four decades of halo masses (and the precision becomes of order 5-10% in the higher mass range). Considering that over this mass range the halo mass function changes by more than three orders of magnitude, this is a non-trivial result.

We also stress that, when comparing our result to the  $N$ -body data as in Fig. 6, we had no freedom of adjusting free parameters. The functional form of the halo mass function was derived from our model, and in this sense it has a different meaning compared to many fitting functions that have been proposed in the literature with the only aim of reproducing the  $N$ -body data. We needed an input from  $N$ -body simulations, namely the scatter of the values of the threshold for collapse, from which we deduced the diffusion coefficient  $D_B$  of the barrier. However, given this input our model makes a prediction for the numerical value of the parameter  $a$  that appears in our halo mass function. This is different from fitting  $a$  directly to the  $N$ -body simulations. The fact that the resulting halo mass function agrees with  $N$ -body simulations much better than the original extended PS theory lends sup-

port to the idea that the diffusing barrier model provides an effective way of including, within the excursion set theory framework, a number of physical effects that are lost when excursion set theory is combined with the simpler spherical or ellipsoidal collapse models.

For precision cosmology, especially in the future, an accuracy such as the one that we have achieved is probably not yet sufficient. Of course, generally speaking, analytic models are not meant to compete with very time-consuming numerical simulations as far as accuracy is concerned. Rather, their role is to provide some physical understanding and some guidance.

However, improvements of the model are certainly possible. In particular, rather than considering a diffusive motion around the constant value  $\delta_c$ , one should consider the actual behavior of the threshold and of its variance with  $\sigma$ . According to Robertson et al. (2008), the average value of the barrier basically follows the prediction (8) of the ellipsoidal collapse, and the scatter around it has a log-normal distribution. In general, fluctuations of the barrier below  $\delta_c$  are rare (the vast majority of points in Fig. 3 of Robertson et al. (2008) lie above  $\delta_c$ , since the average value follows the ellipsoidal collapse barrier, which is a rising function of  $\sigma$ ). However, as we discussed in Section 3, one should not forget that the fluctuations leading to massive clusters are rare events, which belong to the high-mass tail of the distribution function. Since the collapse of a halo depends exponentially on the square of the height of the barrier, even the rare occasional fluctuations that bring the barrier below  $\delta_c$  can end up enhancing significantly the formation probability of the rarest objects. The first-passage time problem with such a stochastic barrier might be hard to solve analytically, but one could simply integrate numerically the corresponding Langevin equation, as in Bond et al. (1991). In the limit of small  $\sigma$  one should recover the results presented in this paper, but for intermediate values of  $\sigma$  there will be corrections. We plan to investigate this issue in future work.

Another possible future development is the investigation of whether universality violations can be accounted for within the excursion set theory framework, supplemented by a stochastic barrier. Recall that, within excursion set theory, the mass function can be written as in eq. (4), where the function  $f$  depends only on the variance  $\sigma$  of the smoothed density field. Thus, this function has a universal form in the sense that its dependence on redshift and on cosmology enters only through the dependence of the variance  $\sigma(R, z)$ . In  $N$ -body simulations there are indications of violations of universality, at approximately 10% level (Reed et al. 2006; Tinker et al. 2008).<sup>7</sup> The evolution with redshift of the exponential cutoff is minimal (Tinker et al. 2008) while a redshift dependence shows up in the coefficients  $a_T$ ,  $b_T$  and  $A_T$  of eq. (41). Since  $c_T$  and therefore our parameter  $a$ , do not show appreciable dependence with  $z$ , within our model these violations of universality cannot be ascribed to a redshift dependence of the diffusion coefficient  $D_B$ . However,  $D_B$  only reflects the scatter of the barrier near  $\sigma = 0$ . In excursion set theory, the  $\sigma$ -dependent prefactors in front of the exponential, in the halo mass function, rather originate from the shape of the ellipsoidal collapse barrier away from  $\sigma = 0$  (Sheth et al. 2001). It would be interesting to study, with  $N$ -body simulations, the

<sup>7</sup> Observe however that these violations of universality depends on the halo finder algorithm, and at least with some halo finders they can be accounted for by systematic corrections due to the finite simulation volume (Lukic et al 2007).

shape and the scatter of the collapse barrier as a function of the redshift at which the halos eventually collapsed and virialized, i.e. to repeat for different  $z$  the analysis performed in Robertson et al. (2008) at  $z = 0$ . One could then generate an ensemble of trajectories by integrating numerically the corresponding Langevin equation, and study when these trajectories first pierce such a stochastic barrier. In this way one could investigate whether excursion set theory supplemented by a stochastic barrier can account for the observed deviations from universality. The interest of such a procedure is that, if this were indeed the case, one would have obtained some insight into the physical mechanisms responsible for the violations of universality. If, in contrast, this procedure should not reproduce the observed universality deviation, one would have to conclude that this is an intrinsic limitation of excursion set theory. In any case, one would get a better understanding of what can, and what cannot, be explained within the framework of this theoretical model.

Finally, another interesting test of our model that could be performed with  $N$ -body simulations is the computation of the barrier scatter, and hence of  $D_B$ , with different halo finders (i.e. with different values of  $\Delta$  in the spherical overdensity algorithm, and with different link-length in the FOF algorithm). Changing the halo finder changes the exponential factor in the mass function, i.e. the constant  $a$ , and the diffusing barrier model predicts that the diffusion coefficient  $D_B$  should change accordingly, in such a way that the relation  $a = 1/(1 + D_B)$  is preserved.

We thank Sabino Matarrese, Ravi Sheth, Cristiano Porciani and Sidney Redner for useful discussions. The work of MM is supported by the Fond National Suisse. The work of AR is supported by the European Community's Research Training Networks under contract MRTN-CT-2006-035505.

## APPENDIX

### A. INCLUSION OF NON-MARKOVIAN CORRECTIONS

In this appendix we compute the effect of the non-markovian corrections due to a tophat filter in coordinate space. As it was shown in paper I, when we use a tophat filter in coordinate space the two-point correlation function can be written as

$$\langle \delta(S_1)\delta(S_2) \rangle = \min(S_1, S_2) + \Delta(S_1, S_2), \quad (\text{A1})$$

where

$$\Delta(S_1, S_2) \simeq \kappa \frac{S_1(S_2 - S_1)}{S_2}, \quad (\text{A2})$$

and  $\kappa \simeq 0.45$ . The first term in the right-hand side of eq. (A1) is responsible for the markovian contribution to the dynamics, and it originates from a Dirac-delta gaussian noise; the second term provides the non-markovian contribution. The reader is referred to paper I for more details.

The fact that the barrier diffuses with a diffusion coefficient  $D_B$  means that

$$\langle B(S_1)B(S_2) \rangle = D_B \min(S_1, S_2). \quad (\text{A3})$$

More generally, even the motion of the barrier can be subject to non-markovian effects, so eq. (A3) should be generalized to

$$\langle B(S_1)B(S_2) \rangle = D_B \min(S_1, S_2) + \Delta_B(S_1, S_2). \quad (\text{A4})$$

Making the rather natural assumption that  $\langle \delta(S_1)B(S_2) \rangle = 0$  and introducing the variable  $X(S) = \delta(S) - B(S)$ , we see that

$$\langle X(S_1)X(S_2) \rangle = (1 + D_B) \min(S_1, S_2) + \Delta(S_1, S_2) + \Delta_B(S_1, S_2). \quad (\text{A5})$$

Thus, our problem becomes formally identical to a problem for a single degrees of freedom  $X(S)$ , with an absorbing boundary condition at  $X = 0$ , with diffusion coefficient  $(1 + D_B)$ , and non-markovianities described by  $\Delta(S_1, S_2) + \Delta_B(S_1, S_2)$ .

We now make the assumption that  $\Delta_B(S_1, S_2)$  is small with respect to  $\Delta(S_1, S_2)$ . This assumption could be tested by extracting the correlator  $\langle B(S_1)B(S_2) \rangle$  from the  $N$ -body simulations, similarly to how the variance  $\langle B^2(S) \rangle$  has been computed in Robertson et al. (2008). The effect of a non-vanishing  $\Delta_B$  can be included perturbatively using the technique that we developed in paper I, just as we did for  $\Delta(S_1, S_2)$ . (Actually, we expect that the two-point function of the critical value for collapse  $B(S)$  receives non-markovian corrections due to the same smoothing procedure that gives the non-markovian corrections to  $\delta(S)$  so, if this is the dominant effect, a plausible expectation is that  $\langle B(S_1)B(S_2) \rangle = D_B [\min(S_1, S_2) + \Delta(S_1, S_2)]$ , i.e. the barrier has the same two-point function as  $\delta(S)$ , apart from the overall diffusion coefficient, so  $\Delta_B(S_1, S_2) = D_B \Delta(S_1, S_2)$ . If this is the case,  $\tilde{\kappa}$  in eq. (35) below is replaced by  $\kappa$ . This would entail a  $\mathcal{O}(25)\%$  modification of the non-markovian correction computed below.)

When  $\Delta_B$  can be neglected, the computation of the halo mass function to first order in the non-markovian corrections can be performed introducing a rescaled "time" variable  $\tilde{S} = (1 + D_B)S$ . Then, using the explicit expression (A2), we get

$$\langle X(\tilde{S}_1)X(\tilde{S}_2) \rangle = \min(\tilde{S}_1, \tilde{S}_2) + \tilde{\kappa} \frac{\tilde{S}_1(\tilde{S}_2 - \tilde{S}_1)}{\tilde{S}_2} \quad (\text{A6})$$

where  $\tilde{\kappa} = \frac{\kappa}{1 + D_B}$ . This is the same problem that we have already solved in paper I, with  $\kappa$  replaced by  $\tilde{\kappa}$  and  $S$  replaced by  $\tilde{S}$ , so the solution can be written immediately, and is given by eqs. (34) and (30).

## REFERENCES

- Audit, E., Teyssier, R. and Alimi, J.-M., 1997, *Astron. Astrophys.* 325,439.  
 Bardeen, J. M., Bond, J. R., Kaiser N. and Szalay, A. S., 1986, *ApJ* 304, 15.  
 Bond, J. R., Cole, S., Efstathiou, G. & Kaiser, N. 1991, *ApJ.* 379, 440.  
 Bond, J. R. and Myers, S. 1996, *ApJS*, 103, 1.

- Dalal, N., White, M., Bond, J. R. & Shirokov, A. arXiv:0803.3453 [astro-ph].
- Desjacques, V., MNRAS 388, 638.
- Doroshkevich, A. G. 1970, *Astrofizika*, 3, 175.
- Grinstein, B., & Wise, M. B. 1986, *ApJ*, 310, 19.
- Grossi, M. et al., arXiv:0902.2013.
- Hänggi, P. 1981, *Z. Phys.* B45, 79.
- Katz, N., Quinn, T. & Gelb, J. M. 1993, *MNRAS*, 265, 689.
- Koyama, K., Soda, J., & Taruya, A. 1999, *MNRAS*, 310, 1111.
- Knessl, C. *et al.* 1986, *J. Stat. Phys.* 42, 169.
- Jeltema, T. E., Canizares, C. R., Bautz, M. W., Buote, D. A, *ApJ* 624, 606
- Jenkins, A. *et al.* 2001, *MNRAS* 321, 372.
- Lam, T. Y., Sheth, R. K. & Desjacques, V., arXiv:0905.1706 [astro-ph.CO].
- Lee, J. & Shandarin, S. F. 1998, *ApJ*, 500, 14.
- Lucchin, F., Matarrese, S., & Vittorio, N. 1988, *ApJ*, 330, L21.
- Lukic, Z., Heitmann, K., Habib, S., Bashinsky, S. and Ricker, P. M. 2007, *ApJ* 671, 1160.
- Lukic, Z., Reed, D., Habib, S. & Heitmann, K. 2009, *ApJ*, 692, 217.
- Maggiore, M. and Riotto, A., arXiv:0903.1249 [astro-ph.CO], (paper I).
- Maggiore, M. and Riotto, A., arXiv:0903.1251 [astro-ph.CO], (paper III).
- Matarrese, S., Lucchin, F., & Bonometto, S. A. 1986, *ApJ*, 310, L21.
- Matarrese, S., Verde, L. & Jimenez, R. 2000, *ApJ* 541, 10.
- Moscardini, L., Matarrese, S., Lucchin, F., & Messina, A. 1991, *MNRAS*, 248, 424.
- Pillepich, A. Porciani, C. & Hahn, O. 2008, arXiv:0811.4176 [astro-ph].
- Press, W. H. & Schechter, P. 1974, *ApJ* 187, 425.
- Redner, S. 2001, "A guide to first-passage processes" (Cambridge University press).
- Reed, D., Bower, R., Frenk, C., Jenkins, A. & Theuns, T. 2007, *MNRAS* 374, 2.
- Robertson, B. et al. 2008, arXiv:0812.3148 [astro-ph].
- Robinson, J., & Baker, J. E. 2000, *MNRAS*, 311, 781.
- Robinson, J., Gawiser, E., & Silk, J. 2000, *ApJ*, 532, 1.
- Sandvik, H. B., Moeller, O., Lee, J. and White, S. D. M. 2006, *MNRAS*, 377, 234.
- Sheth, R. K., Mo, H. J., & Tormen, G. 2001, *MNRAS*, 323, 1.
- Sheth, R. K., & Tormen, G. 1999, *MNRAS*, 308, 119.
- Springel, V. *et al.* 2005, *Nature* 435, 629
- Sugiyama, N. 1995, *ApJS* 100, 281.
- Tinker, J. L. *et al.* 2008, *ApJ*, 688, 709.
- van Kampen N. G. & Oppenheim, I. 1972, *J. Math. Phys.* 13 842.
- van Kampen N. G., 1998, *Braz. Journ. of Phys.* 28 90.
- Warren, M. S., Abazajian, K., Holz, D. E. & Teodoro, L. 2006, *ApJ* 646 881.
- Weiss G. H. et al. 1983, *Physica* 119A 569.
- White, M. 2001, *Astron. Astrophys.* 367, 27.
- Zentner, A. R. 2007, *Int. J. Mod. Phys. D* 16 763.